Journal Pre-proofs

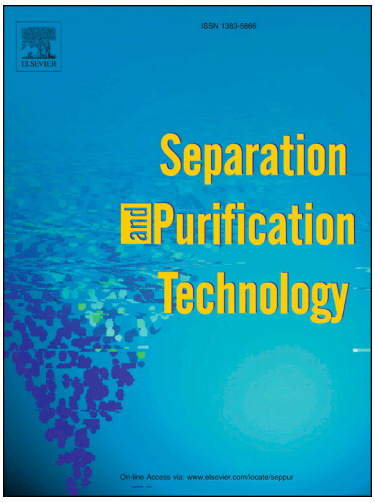

Electrochemical production of extremely high concentrations of hydrogen peroxide in discontinuous processes

Paulo Jorge Marques Cordeiro-Junior, Cristina Sáez Jiménez, Marcos Roberto de Vasconcelos Lanza, Manuel Andrés Rodrigo Rodrigo

PII: S1383-5866(22)01402-2
DOI: https://doi.org/10.1016/j.seppur.2022.121847
Reference: SEPPUR 121847

To appear in: *Separation and Purification Technology*

Received Date: 25 June 2022
Revised Date: 23 July 2022
Accepted Date: 28 July 2022

Please cite this article as: P. Jorge Marques Cordeiro-Junior, C. Sáez Jiménez, M. Roberto de Vasconcelos Lanza, M. Andrés Rodrigo Rodrigo, Electrochemical production of extremely high concentrations of hydrogen peroxide in discontinuous processes, *Separation and Purification Technology* (2022), doi: https://doi.org/10.1016/j.seppur.2022.121847

Electrochemical production of extremely high concentrations of hydrogen peroxide in discontinuous processes

Paulo Jorge Marques Cordeiro-Junior[1,2*]• Cristina Sáez Jiménez[2]• Marcos Roberto de Vasconcelos Lanza[1,*]• Manuel Andrés Rodrigo Rodrigo[2,*]

[1] São Carlos Institute of Chemistry, University of São Paulo (USP), Trabalhador São-carlense street 400, 13566-590, São Carlos, SP, Brazil

[2] Department of Chemical Engineering, Universidad de Castilla-La Mancha, Campus Universitario s/n, 13071 Ciudad Real, Spain

[*]Corresponding authors: manuel.rodrigo@uclm.es

marcoslanza@usp.br

Paulo Jorge Marques Cordeiro-Junior: Conceptualization, Investigation, Methodology, Calculations, Validation, Data curation, Data analyses, Writing - original draft, Writing – review & Editing.

Cristina Saez Jimenez: Conceptualization, Investigation, Methodology, Validation.

Marcos Roberto de Vasconcelos Lanza: Writing Review & Editing, Visualization, Supervision, Project administration, Funding acquisition.

Manuel Andrés Rodrigo Rodrigo: Writing Review & Editing, Visualization, Supervision, Validation, Project administration.

All authors have given their approval for the submission of the final version of the manuscript.

GRAPHICAL ABSTRACT

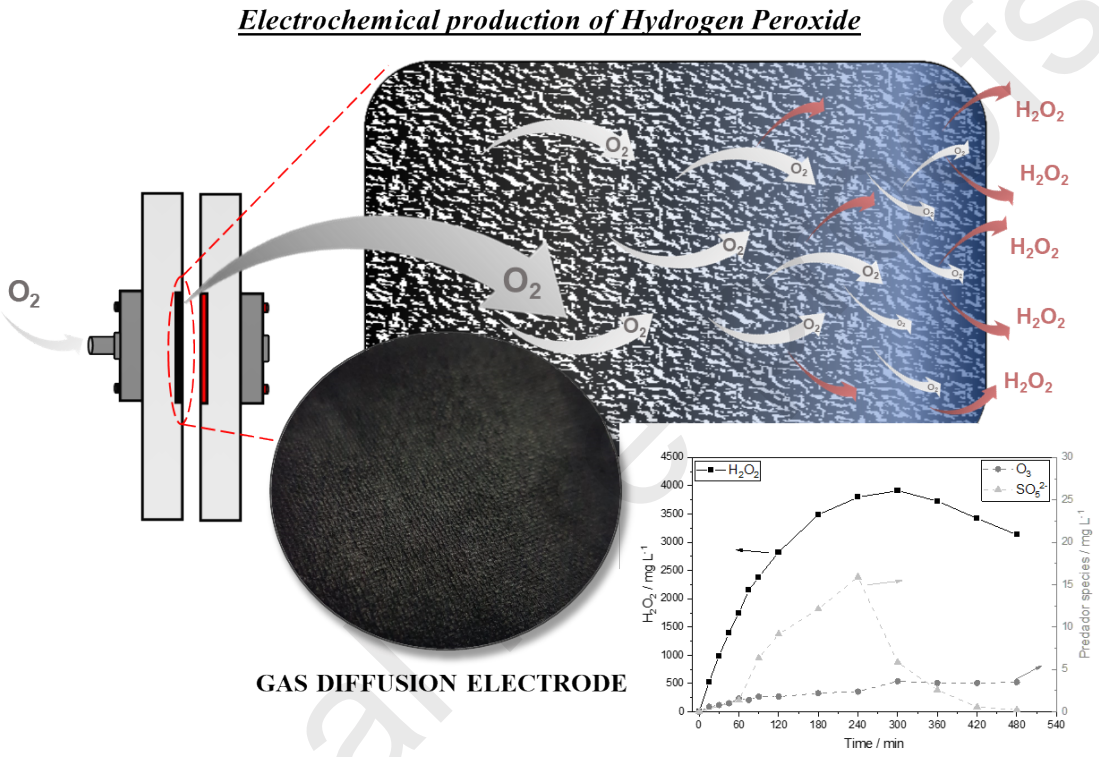

Electrochemical production of extremely high concentrations of hydrogen peroxide in discontinuous processes

Paulo Jorge Marques Cordeiro-Junior[1,2*] • Cristina Sáez Jiménez[2] • Marcos Roberto de Vasconcelos Lanza[1,*] • Manuel Andrés Rodrigo Rodrigo[2,*]

[1] São Carlos Institute of Chemistry, University of São Paulo (USP), Trabalhador São-carlense street 400, 13566-590, São Carlos, SP, Brazil

- Department of Chemical Engineering, Universidad de Castilla-La Mancha, Campus Universitario s/n, 13071 Ciudad Real, Spain

Highlights

- The Printex L6 carbon-based GDE led to the production of an accumulated H_2O_2 concentration in the range of 4,000-5,000 mg/L;
- The Printex L6 carbon-based GDE proved capable of being applied in the industrial-scale production of H_2O_2 using a discontinuous process;
- Improve on H_2O_2 electrosynthesis efficiency of 7.4-36.0 times compared to conventional electrodes and 1.16-11.8 times compared to other GDE-based techniques;
- Printex L6 carbon-based GDE exhibited an H_2O_2 production efficiency of 3.4–3.9 times higher than Vulcan XC-72R carbon-based GDE;
- the GDE showed excellent stability with a lifetime of 36 Ah or 7,5 days of uninterrupted operation

ABSTRACT

This work reports the development and application of a gas diffusion electrode based on Printex L6 carbon for the production of high concentrations of hydrogen peroxide (H_2O_2)

using a flow-by electrochemical reactor in discontinuous operation mode. With the application of current densities ranging between 75 and 200 mA cm^{-2}, the use of Printex L6 carbon-based GDE generated H_2O_2 concentrations in the range of 4,000-5,000 mg L^{-1}, despite the formation of scavengers. The proposed technique also promoted the production of ozone and persulfate species though at low concentrations. The application of the Printex L6 carbon-based GDE led to a roughly 3.4-3.9-fold increase in H_2O_2 concentrations compared to Vulcan XC-72R carbon-based GDE which was used for comparison purposes (Vulcan XC-72R carbon is currently one of the most widely employed carbon materials in electrochemical processes). In addition, the Printex L6 carbon-based GDE exhibited high stability with a lifetime of 36 Ah (7,5 days) of uninterrupted use at 200 mA cm^{-2}. The improvements observed in the Printex L6 carbon-based GDE can be attributed to the presence of higher amounts of carboxyl oxygenated functional groups in the material and its greater electrochemically active surface area compared to the Vulcan XC-72R-based GDE.

Keywords: Hydrogen peroxide; Oxygen reduction reaction; Gas diffusion electrode, amorphous carbon; Electrochemical production of hydrogen peroxide

1 Introduction

Currently, hydrogen peroxide (H_2O_2) is one of the most powerful and eco-friendly chemical oxidants that are widely employed in the world. Annually, nearly 4 million tons

of H_2O_2 are consumed worldwide, and this value is estimated to rise to 6 million tons by 2027 [1–4]. The high consumption of H_2O_2 can be explained in terms of its wide range of industrial applications; the oxidant is commonly applied in paper bleaching, wastewater

treatment, and as cleaning agent, among other uses[2,5–7]. Recently, as part of the efforts to combat SARS-CoV-2 (COVID-19), H_2O_2 has also been employed as a reagent for the formulation of products used for decontaminating surfaces and for the disinfection of N95 masks for reuse [6].

Currently, most of the industrial-scale global production of H_2O_2 is conducted by the anthraquinone oxidation process (AOP), which was first reported in 1939 by Rleidl and Pfleiderer[1,3,4,6]. This process has become widely popular because its application leads to the production of large amounts of H_2O_2. However, in spite of the high efficiency of the AOP in terms of H_2O_2 production, the technique involves an energy-intensive multi-step mechanism [1,3]; apart from that, the process has other non-negligible disadvantages which include the following: the need for H_2O_2 purification, storage and transport (as it is not easy to be produced in-situ), in addition to the massive amount of wastes generated in the process [1,3]. To tackle these underlying problems, several studies have proposed the use of highly efficient in-situ H_2O_2 production-based techniques. One of such techniques that has gained enormous traction among researchers in recent years involves H_2O_2 production from oxygen electroreduction reaction (ORR); this technique has become widely popular due to its high efficiency and operational safety[7–12]. Under the ORR technique, when acid medium is applied, O_2 is reduced to H_2O_2 on the cathode surface of an electrochemical cell; the process involves the transfer of 2 electrons, as can be observed in Equation (1)[7,11–14].

$$O_2 + 2\,H^+ + 2\,e^- \rightarrow H_2O_2 \qquad (E^0 = 0.682\ \text{V}\ vs.\ \text{SHE}) \qquad (1)$$

Carbon-based materials are known to exhibit excellent performance when applied as cathodes for the electrosynthesis of H_2O_2; this excellent performance can be attributed to the following outstanding properties of these materials: abundant availability, low cost, non-toxic behavior, excellent conductivity, and high surface area[4,7,11,15]. In fact, different kinds of carbon-based materials, including graphite, graphene, carbon nanotubes, reticulated vitreous carbon, and carbon black, have already been applied for H_2O_2 electrosynthesis, where they have either been employed alone or in combination with other materials [8,16–18]. The main shortcomings of the electrochemical processes are related to mass transport which stems from the extremely low solubility of oxygen (the raw material in the electrochemical process) [19]; this mass transport constraint causes low H_2O_2 production efficiency in electrochemical processes.

Table 1 presents some recent studies reported in the literature related to the electrochemical production of hydrogen peroxide, the technique applied and the production energy efficiency obtained (this is largely influenced by the technique adopted) – which ranges between 9 and 135 g per kWh. The concentrations of H_2O_2 obtained during electrolysis in discontinuous mode are limited by the electrochemical decomposition of the oxidant, which directly depends on the concentration of hydrogen peroxide accumulated in the electrolyte; in other words, there is always a value at which the production and decomposition rates balances and this value corresponds to the maximum concentration of hydrogen peroxide that can be obtained under the operating conditions. In addition, depending on the electrochemical cell configuration, scavengers, such as peroxosulfates or ozone, can be produced, and in this case, the production of hydrogen peroxide over time does not become stabilized but rather declines when high current charges are applied.

Table 1. Production of H_2O_2 in ORR via 2-electron pathway in the literature.

Cathode composition	Operating condition	[H_2O_2] accumulation mg L^{-1} (mmol)	H_2O_2 production energy efficiency g kWh^{-1}	[ref]
Graphite felt (GF)	0.05 M Na_2SO_4, pH 7, 50 mA cm^{-2}, 60 min	108	---	[16]
Carbon black/PTFE/GF	0.05 M Na_2SO_4, pH 7, 50 mA cm^{-2}, 60 min	473 (0.001)	---	[18]
Graphene/carbon black/PTFE/GF	0.05 M Na_2SO_4, pH 7, 0.9 V, 120 min	525 (1.5)	97.2	[17]
Carbon black/PTFE	0.05 M Na_2SO_4, pH 3, 5 mA cm^{-2}, 480 min	300 (23.8)	101.3	[8]
Carbon black/PTFE	0.05 M Na_2SO_4, pH 3, 5 mA cm^{-2}, 480 min	400 (31.8)	135.0	[20]
Gas diffusion electrode				
Graphene/PTFE GDE	0.05 M K_2SO_4, pH 3, 29 mA cm^{-2}, 180 min	495 (5.8)	15.2	[21]
Carbon black/PTFE GDE	0.1 M K_2SO_4, pH 2.5, 50 mA cm^{-2}, 90 min	755 (5.5)	23.3	[22]
Sudan Red-Carbon black/PTFE GDE	0.1 M K_2SO_4/ H_2SO, 100 mA cm^{-2}, 90 min	1025 (7.5)	9.5	[23]
Co-Carbon black/PTFE GDE	0.1 M K_2SO_4/ H_2SO_4, -0.9 V, 90 min	331 (2.4)	12.5	[9]
Co-Carbon black/PTFE GDE	1 M KOH, -1.1 V, 300 min	6,424 (75.6)	28.0	[24]

Over the past few years, significant progress has been made in the development of highly efficient electrochemical techniques which have been capable of generating large concentrations of hydrogen peroxide. Yu et al. (2014; 2015) obtained accumulated H_2O_2 concentrations ranging from 108 to 473 mg L^{-1} based on the application of graphite felt (GF) and carbon black/PTFE-GF, respectively, in 60 min of electrolysis[16,18]. Other studies employed pressurization and flow-through electrodes to help circumvent the

problems related to low solubility of O_2 in the electrochemical process; these techniques led to the electrosynthesis of higher H_2O_2 concentrations with greater current efficiencies [8,20]. It should be noted that the conventional way to address the problem related to low solubility of O_2 is via the use of gas diffusion electrode (GDE)[9,10,22–26]. Owing to the highly porous 3D structure of GDE, the use of this electrode has been found to lead to relatively higher efficiency compared to flat electrodes [10,24,25]. Furthermore, the use of GDE helps overcome the constraints related to low solubility of O_2 and allows a high amount of O_2 molecules to reach the ORR active sites located on the electrode surface[9,24,25].

Previous studies reported in the literature which involved the use of GDE composed of graphene [21], carbon black [22,26], and modified carbon black [9] obtained accumulated H_2O_2 concentrations ranging from 495 to 755 mg L^{-1} in less than 90 min of electrolysis. Interestingly, the application of Printex L6 carbon-based technique for the generation of hydrogen peroxide led to the production of substantially higher H_2O_2 concentrations where accumulated H_2O_2 concentrations as high as 6424 mg L^{-1} were obtained in 300 min of electrolysis under extremely alkaline medium [24]; remarkably though, the use of high-carbon loading under this extremely alkaline medium caused a drastic reduction in the lifetime of the carbon-based electrodes (nearly 3 times worse than in acidic media[27,28]. Taking the above considerations into account, we sought to tackle the problems related to short lifetime of the electrode and high carbon loading in the catalyst by evaluating the use of Printex L6 carbon under different conditions. Thus, the present study reports the development and application of a novel GDE composed of Printex L6 carbon film supported on carbon cloth for the production of H_2O_2 through ORR via 2-electron pathway in an acidic medium using a flow-by electrochemical reactor. For a thorough analysis of the efficiency of the Printex L6 carbon-based GDE in

the electrogeneration of H_2O_2, the cathode material was compared with Vulcan XC-72R carbon - a typical standard material which has been employed in several works reported in the literature and regarded as one of the most efficient carbonaceous materials used in electrochemical processes.

2 Experimental

2.1 Electrode preparation

The catalytic mass was prepared by mixing Printex L6 carbon – PL6C (Evonik) or Vulcan XC72R carbon (Cabot) with 20% of PTFE (w/w) in ultrapure water and stirring the mixture constantly for 1 h. 10 g of the wet mass was evenly spread over the carbon cloth (126 cm^2), which was then heated at 120 °C for 15 min (to remove the excess of water). Subsequently, the electrode was hot-pressed at 5 tons under 290 ºC for 2 h. The electrode was cut in the shape of a circle with geometric surface area of 20 cm^2.

2.2 Electrochemical Study

Electrochemical studies were carried out in a flow-by electrochemical reactor using a dimensionally stable anode (DSA®-Cl_2) as anode and a gas diffusion electrode as cathode (geometric area of both electrodes: 20 cm^2). The undivided electrochemical cell contains an 8 mm separator between the electrodes. O_2 flow of 50.0 mL min^{-1} was applied in the cathode compartment. Ag/AgCl 3.0 M. was employed as pseudo-reference electrode. The pump was operated at a flow rate of 50.0 L h^{-1} and the experiments were conducted using 0.1 mol L^{-1} Na_2SO_4 (pH 2.5 adjusted with H_2SO_4 - the pH was controlled during the experiments, even though no changes were observed) as electrolyte solution. The total volume of electrolyte used was 1.0 L at a controlled temperature of 15.0 ºC, and this was maintained during the operation using a cooling system.

The experiment involving the electrogeneration of hydrogen peroxide was conducted in an Autolab PGSTAT302N potentiostat coupled to a high current unit

(BOOSTER BSTR-10A) using constant current densities of 75, 150 and 200 mA cm^{-2}. The H_2O_2 electrogenerated was quantified by UV-Vis spectrometry using the titanium (IV) oxysulfate method. Aliquots of 0.5 mL were collected during the electrolysis and

were added to a solution containing 5 mL of $TiOSO_4$. The quantification of H_2O_2 was carried out by measuring the absorbance at a wavelength of 408 nm using Agilent 300 Cary series UV-Vis spectrophotometer.

Cyclic voltammetry studies were performed under wide potential window (1.0 to -0.8 V) and cathodic potential window (0.0 to -0.8 V) at different scan rates (2.5; 5.0; 10; 25; 50; 75 and 100 mVs^{-1}) in order to determine the specific electrochemical area of the electrodes (ECSA). The durability of the electrodes was evaluated using a single compartment cell in O_2–saturated 0.1 mol L^{-1} Na_2SO_4 (pH 2.5 adjusted with H_2SO_4). The lifetime of the electrode was evaluated using Arbin Instruments (model FBTS – 20V) at the current density of 200 mA cm^{-2}. Cyclic voltammetry analysis was performed in the potential window of 1.0 to -0.8 V and 0.0 to -0.8 V, at scan rate of 50 mV s^{-1} using an Autolab PGSTAT302N before and after the electrochemical durability tests.

2.3 Morphological and structural characterization

The Printex L6 and Vulcan XC72 carbon-based electrodes were morphologically characterized by scanning electron microscopy (SEM) using HRSEM-Gemini-500 equipment. The surface area was determined by BET analysis using Micromeritics Asap 2010 equipment, and XPS analysis was carried out using PHOIBOS 150 9MCD Power Analyzer (SPECS) with an X-ray power source (Mg non-monochromatic) operating at 200 W and 12 kV.

3 Results and discussion

3.1 Electrosynthesis of H_2O_2 with PL6C-based GDE: general behavior

the Printex L6 carbon-based GDE in a flow-by electrochemical reactor, electrolysis tests were performed at the constant current density of 150 mA cm^{-2}. Figure 1 shows the concentration of H_2O_2 electrogenerated over time. One will observe that there is a linear increase in the production of H_2O_2 during the first hour of electrolysis; this result points to pseudo-zero order kinetics, where the apparent kinetic constant value = 29.1 mg L^{-1} min^{-1}. The kinetic constant value obtained clearly pointed to the high efficiency of the technique in terms of H_2O_2 production, where a maximum H_2O_2 concentration of above 3,900 mg L^{-1} was generated in 5 h. The amount of H_2O_2 concentration generated under the proposed technique was found to be higher than the values reported in other studies published in the literature (see Table 1); the application of the Printex L6 carbon-based GDE led to an improved efficiency (in terms of H_2O_2 electrogeneration) of 7.4-36.0 times compared to flat or conventional electrodes and approximately 1.16 to 11.8 times in relation to other GDE-based techniques.

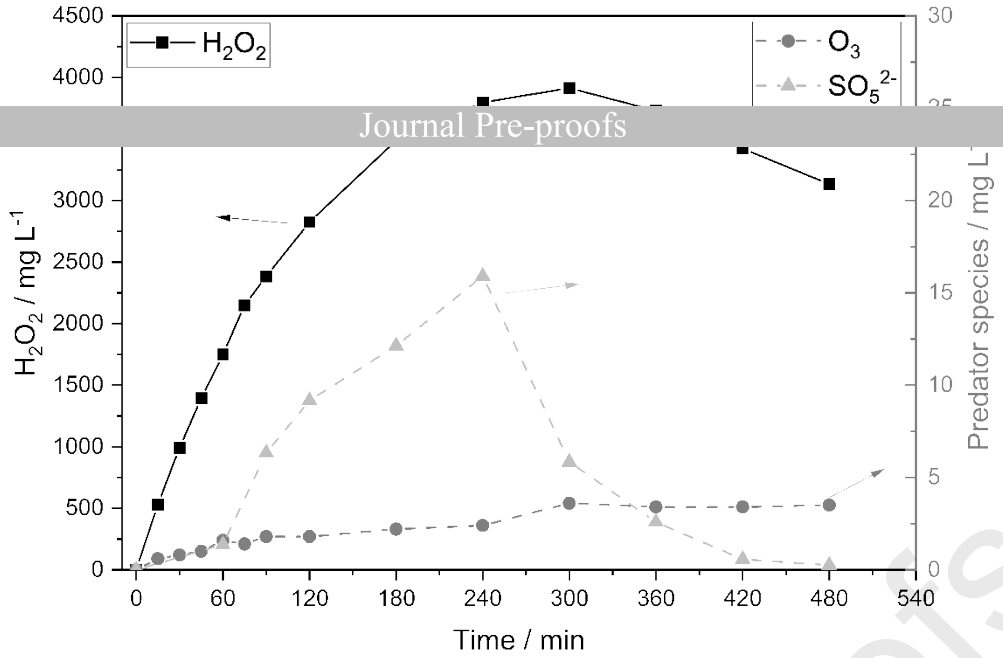

Figure 1. Amounts of electrogenerated H_2O_2, O_3, and SO_5^{2-} in mg L^{-1} based on the application of the Printex L6 carbon-based GDE in electrolysis at the current density of 150 mA cm^{-2} using 0.1 mol L^{-1} Na_2SO_4, at pH 2.5, as supporting electrolyte.

Apart from the production of H_2O_2, the application of the PL6C/GDE-based electrochemical technique also led to the formation of ozone (O_3) and persulfate (SO_5^{2-}) species in lower concentrations, with maximum values of 4.0 mg L^{-1} O_3 and 15.9 mg L^{-1} SO_5^{2-} generated in 480 min and 240 min of electrolysis, respectively. Ozone can be generated in electrochemical reactors from the electrolysis of water on the anode surface via 6-electron transfer mechanism, as can be observed in Equation (2). This process is known as electrochemical ozone production (EOP). In addition, peroxymonosulfate can also be generated on the anode, based on Equation (3)[5,29–33].

$$3H_2O \rightarrow O_3 + 6H^+ + 6e^- \quad (2)$$

$$H_2O + SO_4^{2-} \rightarrow 2H^+ + 2e^- + SO_5^{2-} \quad (3)$$

Both O_3 and SO_5^{2-} are considered predator species of H_2O_2 - see Equations (4) and (5) [5,29–33]. Thus, as both predator species increase, the concentration of H_2O_2 tends to

decrease; this was observed by the decrease in H_2O_2 production after 5 h of electrolysis. The maximum concentration of SO_5^{2-} species was recorded in 240 min of electrolysis; after that, a decrease was observed in its concentration. This outcome shows that SO_5^{2-} reacts with H_2O_2 (Equation 5) or with O_3 (Equation 6).

$$H_2O_2 + O_3 \rightarrow 2O_2 + H_2O \quad (4)$$

$$H_2O_2 + SO_5^{2-} \rightarrow 2O_2 + H_2SO_4 \quad (5)$$

$$O_3 + SO_5^{2-} \rightarrow 2O_2 + SO_4^{2-} \quad (6)$$

Based on these observations, it is clear that the decline observed in the concentration of hydrogen peroxide is attributed to the interaction of this oxidant with other oxidants electrogenerated simultaneously in the electrochemical process. It is important to bear in mind that in the absence of other predators, the concentration of hydrogen peroxide would not have decreased but stabilized at a value where the rates of production and decomposition of H_2O_2 would be in equilibrium on the anode[9,24,25]; this behavior has been described in the electrosynthesis of many other oxidants in discontinuous processes. The H_2O_2 decomposition reactions can be both: i) decomposition of H_2O_2 at the anode surface with formation of O_2 and H_2O, according to Equation 7; and ii) self-decomposition of H_2O_2 within the solution, Equation 8.

$$H_2O_2 \rightarrow O_2 + 2H^+ + 2e^- \quad (7)$$

$$2H_2O_2 \rightarrow O_2 + 2H_2O \quad (8)$$

3.2 Printex L6 vs Vulcan XC72R

To evaluate the efficiency of the PL6C-based GDE in H_2O_2 electrosynthesis, a comparative analysis was conducted using the proposed material (PL6C/GDE) and Vulcan XC-72R carbon-based GDE under the following constant current densities: 75, 150, and 200 mA cm^{-2}. Vulcan XC72-R carbon is one of the most widely employed amorphous carbon-based supporting materials for the preparation of catalysts; this

material has been extensively applied not only for the catalysts used in hydrogen peroxide production but also for the preparation of catalysts used in fuel cells [11,34]. As pointed out by Assumpção[11], Vulcan XC-72R carbon is regarded as one of the best commercial

electrocatalyst supporting materials because of its excellent properties, which include high surface area (250 m^2 g^{-1})[11,34], good average particle size (50 nm), and excellent electrical conductivity (4.5 S cm^{-1})[34]. For comparison purposes, Printex L6 carbon (PL6C) is another type of commercial amorphous carbon which has properties that are quite similar to Vulcan XC-72R carbon; PL6C has a surface area of 265 m^2 g^{-1}, an average particle size of 35 nm [7,11,12], and electrical conductivity of 3.3 S cm^{-1} [34].

As can be seen in Figure 2A, compared to Vulcan XC-72R/GDE, the PL6C/GDE exhibited better performance in terms of H_2O_2 electrosynthesis in ORR via $2e^-$; the application of the PL6C/GDE under galvanostatic experimental operation yielded maximum H_2O_2 concentrations of 4616 mg L^{-1} (12h), 3913 mg L^{-1} (5h), and 5032 mg L^{-1} (4h) at the current densities of 75, 150 and 200 mA cm^{-2}, respectively, while Vulcan XC72R/GDE recorded maximum H_2O_2 concentrations of 2170 mg L^{-1} (8h), 799 mg L^{-1} (4h), and 625 mg L^{-1} (1.5h), at the same respective current densities.

The apparent kinetic constant (k_{app}) value for each current density was also estimated. The Vulcan XC-72R/GDE recorded k_{app} values of 10.43, 8.57, and 9.49 mg L^{-1} min^{-1}, while the PL6C/GDE recorded k_{app} values of 16.52, 29.08, and 41.04 mg L^{-1} min^{-1} at current densities of 75, 150 and 200 mA cm^{-2}, respectively, in the first 5 Ah (ampere hour) of operation. It is worth mentioning that at the current density of 75 mA cm^{-2}, no significant decrease in H_2O_2 concentration was observed because the generation of persulfate and ozone predator species was effectively inhibited; this usually occurs at higher current densities as this condition leads to the production of low amount of hydroxyl radicals on the anode surface. It should be noted that the application of milder

conditions is likely to prevent the formation of hydroxyl radicals on the surface of the anode[35]this, in turn, is expected to inhibit the formation of both predator species.

The effects of current density using carbon-based GDE have been reported in some works. In most, it is shown that the effect of increasing current density (j) increases the production of H_2O_2 until a maximum concentration is reached at an ideal current density. Moreira et al (2019) showed that with the increase of j the production of H_2O_2 until the value of 100 mA cm^{-2}, from this value of current density, the production of H_2O_2 decreased by 200 mg L^{-1} [23]. In turn, the results of H_2O_2 production by applied current density reported by Lima et al showed that the ideal condition was 75 mA cm^{-2} producing an H_2O_2 concentration of 755 mg L^{-1} in 90 min of electrolysis [22]. This effect occurs because, with the increase in the current density, there is an increase in the parallel reactions, such as (i) ORR via 4-electrons, yielding H_2O as a product (Equation 9); and (ii) hydrogen evolution reactions (Equation 10).

$$O_2 + 4\,H^+ + 4\,e^- \rightarrow H_2O \quad (9)$$

$$2\,H^+ + 2\,e^- \rightarrow H_2 \quad (10)$$

Thus, high current density values are not ideal to be used in 2-electron ORR studies with GDEs. In contrast, in our previous work [36], different current densities were evaluated (25 to 200 mA cm^{-2}), and it was observed that as the current density increased, the electrochemical production of H_2O_2 also increased, which was not possible to observe an ideal current density. This effect was also observed by Zhang et al (2020), in which the increase in current density up to 240 mA cm^{-2} also only tended to increase the production of H_2O_2 [37].

As can be observed in Figure 2B, the cathode potential ($E_{cathode}$) and cell potential (E_{cell}) values recorded for Vulcan XC-72R carbon were very similar to those of Printex L6 carbon; this shows that both materials operate under similar electrochemical

conditions. This observation is clearly in line with what is expected, since both materials present almost similar levels of electrical conductivity.

In terms of maximum efficiency of H_2O_2 production (the figure of merit found to be more reliable in real applications once it takes into account cell voltage when analyzing the efficiency of electrochemical processes in terms of the amount of H_2O_2 produced in g per kWh used), PL6C exhibited maximum production efficiency of 17.8 g kWh^{-1}, which was 4-times higher than Vulcan XC-72R at both current densities of 150 and 200 mA cm^{-2} (higher current densities); this result evidently points to the greater efficiency of the PL6C material. At the current density of 75 mA cm^{-2}, the PL6C/GDE exhibited an increase in H_2O_2 production efficiency of up to 29.5 g kWh^{-1}; this value was 1.5-fold higher than the value recorded for Vulcan XC-72R/GDE. Table 1 shows the results of efficiency of H_2O_2 production obtained in other works reported in the literature, and it can be used to compare with the values obtained in the present work. As can be observed, the (H_2O_2) production efficiency values obtained for the PL6C/GDE were found to be close to the values recorded for other GDE-based techniques proposed in other studies. It is worth pointing out however that the production efficiency values obtained in our present study were found to be much lower than those reported by studies that employed flat electrodes and/or flow-through electrochemical cells; this can be primarily attributed to the electrochemical cell configuration which is allowed to operate at lower current densities while the ohmic resistance is minimized by the small distance separating the cathode from the anode, leading to lower cell potential values. In GDE-based flow-by systems, the distance between the electrodes cannot be too small as this leads to the formation of bubbles and air on the cathode surface. It should be noted that the use of flow-by cells does not lead to the formation of scavengers and allows the accumulation of higher concentrations of hydrogen peroxide during operation in discontinuous mode.

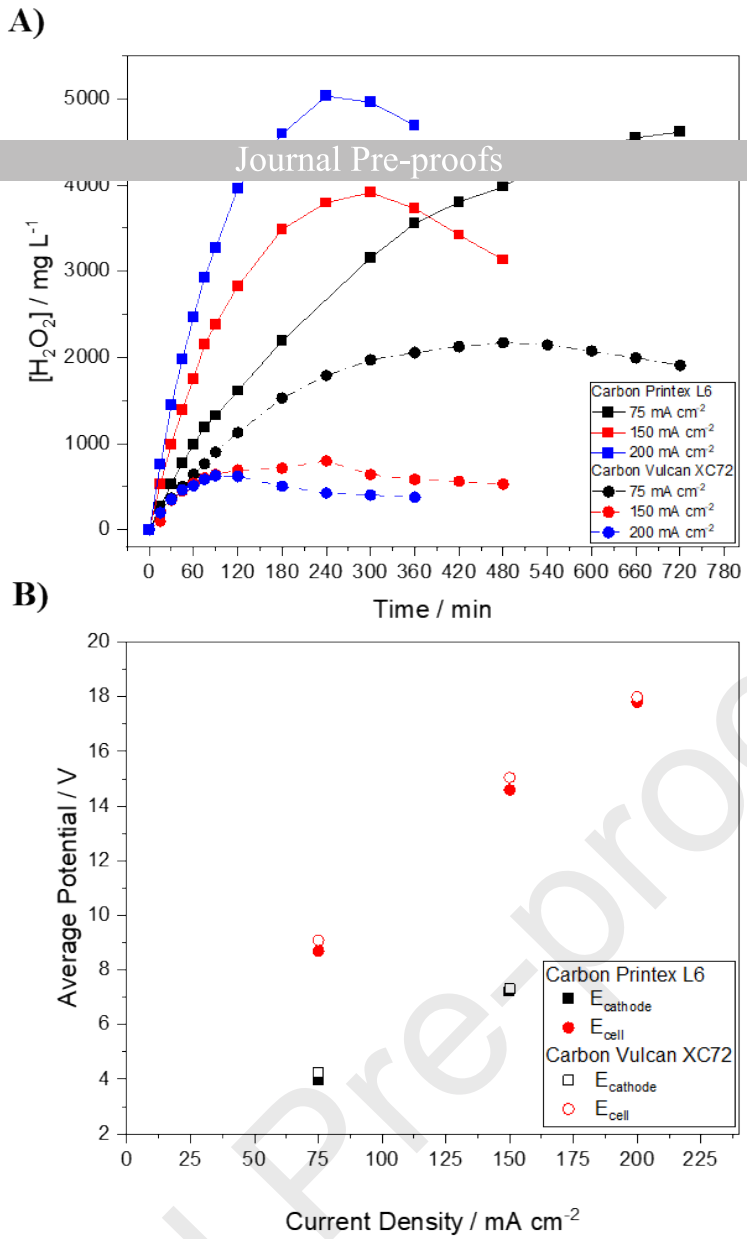

Figure 2. A) Amount of H_2O_2 electrogenerated in mg L^{-1} as a function of time and **B)** average cell and cathode potential for Printex L6 carbon and Vulcan XC-72R carbon in electrolysis conducted at the current densities of 75, 150, and 200 mA cm^{-2} using 0.1 mol L^{-1} Na_2SO_4, at pH 2.5, as supporting electrolyte.

A relevant observation that deserves being mentioned is that even though the PL6C/GDE and Vulcan XC-72R/GDE initially exhibited similar electrochemical behavior, the results obtained from the application of the electrodes under the same experimental conditions showed that the former recorded nearly 3.4–3.9-fold increase in H_2O_2 electrogeneration compared to the latter. Thus, the type of amorphous carbon

employed in the GDE is one of the key factors that exert an influential role on the electrogeneration of H_2O_2. According to reports in the literature[4,7], the high performance of amorphous carbon can be attributed to the following factors: i) degree of aromaticity; ii) oxygenated functional groups on the surface; iii) pore structure size; and iv) surface area.

The degree of aromaticity is largely dependent on the amount of sp^2 and sp^3 carbon in the structure of the amorphous carbon material. Higher sp^2 carbon contents favor electrical conductivity because of the presence of unpaired electrons and $\pi - \pi^*$ transitions, while higher sp^3 carbon contents cause defects and edges in the material structure and this may contribute toward enhancing the performance of ORR due to the generation of a larger number of active sites on the electrode surface [12,15,34,38]. The deconvoluted C1s spectra (Figure 3) of both amorphous carbon materials (PL6C and Vulcan XC-72R) show the presence of a more intense peak at 284.5 eV which corresponds to the C=C sp^2 bond for Vulcan XC-72R carbon (53.1 % peak area for Printex L6 carbon and 50.8% for Vulcan XC-72R carbon). Considering that Vulcan XC-72R carbon is characterized by the presence of $\pi - \pi^*$ transitions (at 291.2 eV); this was not observed for Printex L6 carbon. In fact, the similar value in the sp2/sp3 ratio between the two carbon materials (of 1.6) indicates that both materials have similar conductivity properties, and consequently operate on the same electronic behavior, which was observed in the values of E_{cell} and $E_{cathode}$, as can be seen in Figure 2B.

Both carbons materials had similar contents of oxygenated functional groups (14.7 % for Printex L6 carbon and 14.5 % for Vulcan XC-72R carbon). The C1s and O1s spectra in Figure 3 show that both carbon materials exhibit the same types of oxygenated functional groups: carbonyl (C=O) and carboxyl (O–C=O) groups, at 287.5 and 289.3 eV, respectively. Remarkably, the carbonyl peak intensity recorded for Printex L6 carbon was

found to be almost twice as high as that of Vulcan XC-72R carbon. Printex L6 carbon presented mostly the carboxyl functional group with a peak area of 14.5 %; while the Vulcan XC-72R carbon presented the carbonyl functional group with a peak area equal to 10.8 %, as can be seen in Table 2.

As reported in the literature, the presence of oxygen-containing functional groups in the carbon surface, especially the carboxyl group (O–C=O), are found to enhance ORR efficiency; this is because the presence of the carboxyl group in the vicinity of the ORR active site on the carbon structure boosts the formation of OOH* reaction intermediate and the adsorption of O_2 molecule, and this favors H_2O_2 electrosynthesis [7]. This effect is more pronounced for the carboxyl functional group than for the carbonyl functional group [6,39,40]. Therefore, the presence of higher contents of carboxyl functional groups in Printex L6 carbon (14.5 % of O–C=O-content in PL6C compared to 3.70% in Vulcan XC-72R carbon) shows that this carbon material has a suitable chemical structure that is more favorable for H_2O_2 electrosynthesis compared to Vulcan XC-72R carbon [11].

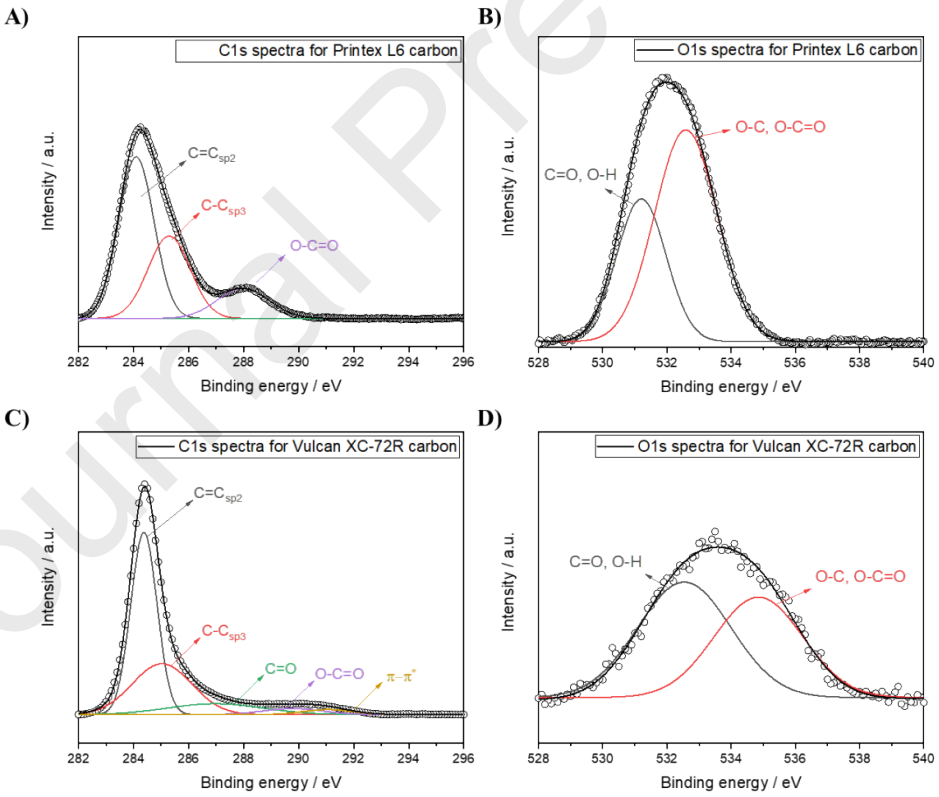

Figure 3. C1s**(A)** and O1s **(B)** spectra for Printex L6 carbon; C1s **(C)** and O1s **(D)** spectra for Vulcan XC-72R carbon.

Table 2. Relative peaks areas of each functional group and elements contents (%) in carbon (C1s) and oxygen (O1s) spectra.

	Area of C 1s peaks (%)					Element content	
Sample	**C=C_{sp2}**	**C–C_{sp3}**	**C=O**	**O–C=O**	**π–π^***	**C (%)**	**O (%)**
Printex L6	53.1	32.2	0.2	14.5	----	85.3	14.7
Vulcan XC-72R	50.8	32.0	10.8	3.7	2.6	85.5	14.5

As previously mentioned, the last two parameters that may affect the performance of amorphous carbon materials when it comes to H_2O_2 production are particle size and surface area. Figure 4 shows the SEM images of Printex L6 carbon and Vulcan XC72 carbon with 25,000x magnification. Both films can be found to be characterized by a highly porous morphology formed by agglomerated particles, with average particle size distribution of 44.6 nm and 81.64 nm for Printex L6 carbon (Figure 2C) and Vulcan XC72 carbon (Figure 2D), respectively. The size distribution profile of the SEM images was obtained using the Image J software.

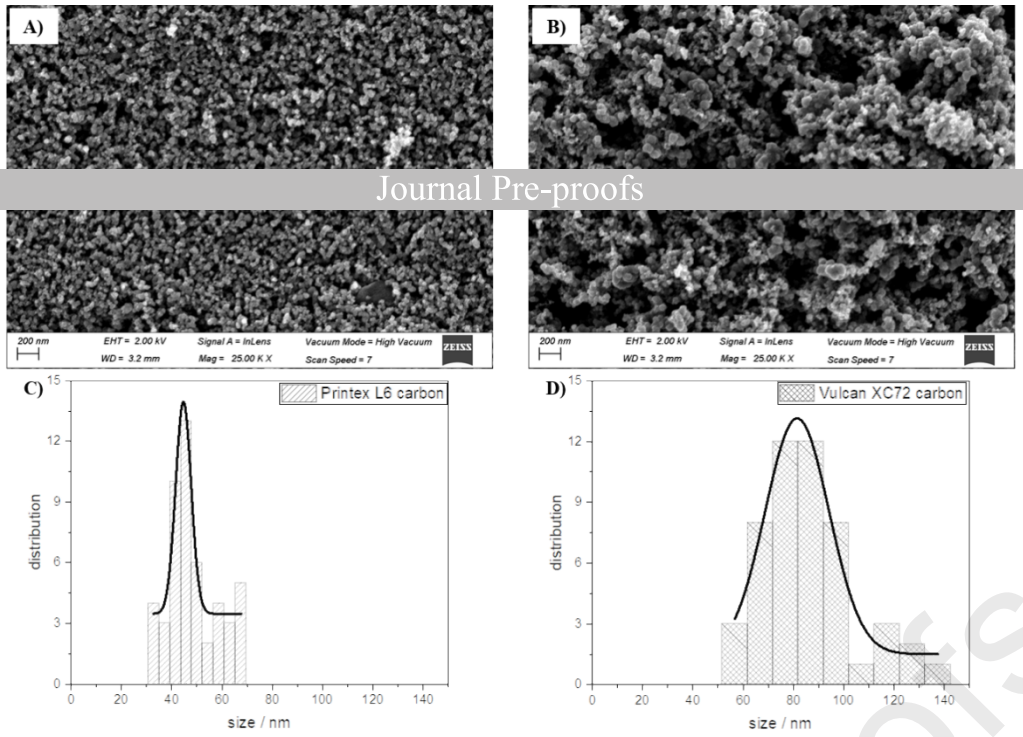

Figure 4. SEM images of **A)** Printex L6 carbon and **B)** Vulcan XC72 carbon incorporated into the GDE with 25000x magnification. Particle size distribution for **C)** Printex L6 carbon and **D)** Vulcan XC72 carbon incorporated into the GDE.

When the carbon material is incorporated into the GDE, the particle size increases in both cases because the PTFE agglomerates the carbon particles into larger particles. Interestingly, Printex L6 and Vulcan XC-72R carbon in powder have very similar surface area by B.E.T. analysis (see Table 3); while the B.E.T. surface area decreases significantly when the carbon material is incorporated into the GDE, though the difference (in B.E.T surface) between the two carbon materials remains in the same order of magnitude, as shown in Table 3.

Table 3. Data obtained related to average particle size and BET surface area for Printex L6 carbon and Vulcan XC-72R.

	Average particle size		B.E.T surface area*	
	in powder*	**on the GDE**	**in powder***	**on the GDE**
Printex L6 carbon	35	44.6	265	68.54 ± 0.17
Vulcan XC-72R carbon	50	81.6	250	52.81 ± 0.48

* data informed by the manufacturer.

Because the surface area and particle size distribution values obtained for the two amorphous carbon materials are very similar, the best way to verify the morphological effect is through the measurement of the electrochemically active surface area (ECSA). The ECSA for the two GDE-based catalysts was calculated using the electrical double layer capacitance of the catalytic surface (C_{dl}). To this end, cyclic voltammetry (CV) analysis was carried out under the following conditions: i) in a wide potential range ranging from +1.0 to -0.8 V (vs Ag/AgCl 3M) – see Figures 5A and B; and ii) in the cathodic potential range ranging from 0.0 to -0.8 V – see Figures 5C and D.

As can be seen in the CV profiles shown in Figure 5, both carbon materials (PL6C and Vulcan XC-72R) exhibited high current values; these results are linked to the redox reaction of the oxygen-containing functional groups, including the carbonyl and carboxyl groups (as previously discussed using the XPS data). The current values obtained for the Printex L6 carbon-based GDE were approximately 1.72 times higher than the values obtained for Vulcan XC-72R carbon-based GDE; this was precisely due to the presence of relatively higher contents of oxygenated groups on the PL6C surface. Another relevant observation that deserves to be highlighted in Figures 5C and D is that the ORR onset potential starts earlier for the Printex L6 carbon-based GDE; this difference of about 150 mV in ORR onset potential shows that Printex L6 carbon exhibits a higher ORR

electrocatalytic activity than Vulcan XC-72R carbon - this can be found better illustrated in Figure 6.

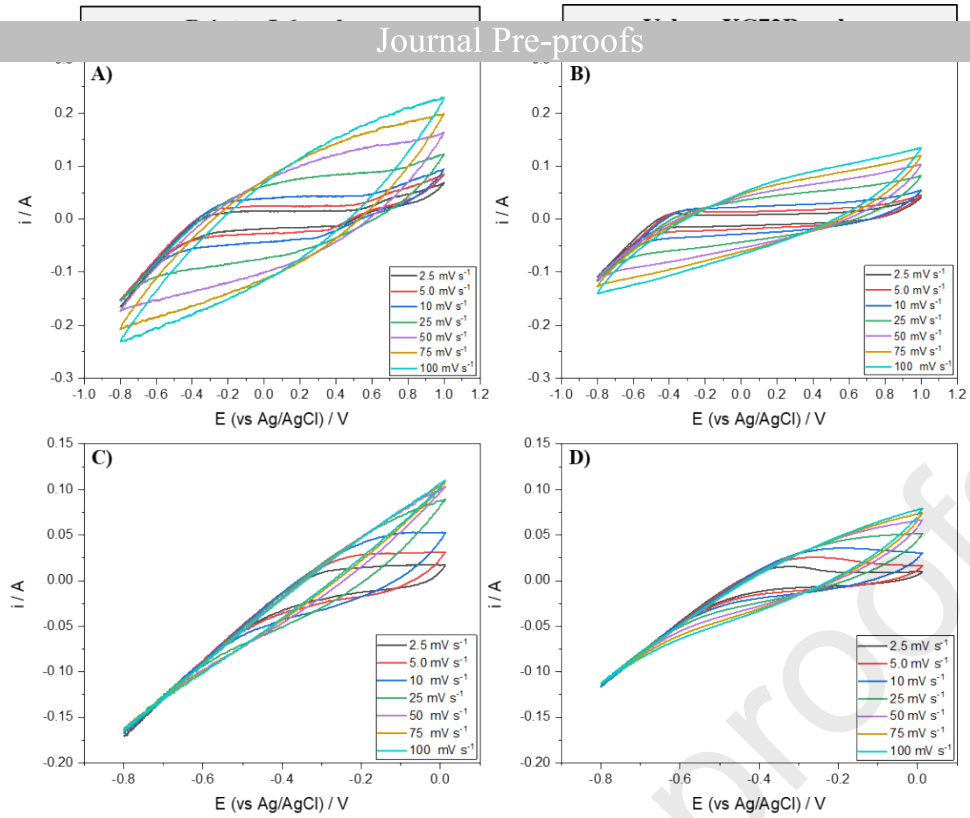

Figure 5. Cyclic voltammetry curves obtained under the potential ranging from +1.0 to -0.8 V for **A)** Printex L6 carbon and **B)** Vulcan XC72 carbon; and in the potential ranging from 0.0 to -0.8 V (cathodic region) for **C)** Printex L6 carbon and **D)** Vulcan XC72 carbon. The analysis was conducted using O_2-saturated 0.1 mol L^{-1} Na_2SO_4 (pH 2,5 adjusted with H_2SO_4) as electrolyte solution and different scan rates.

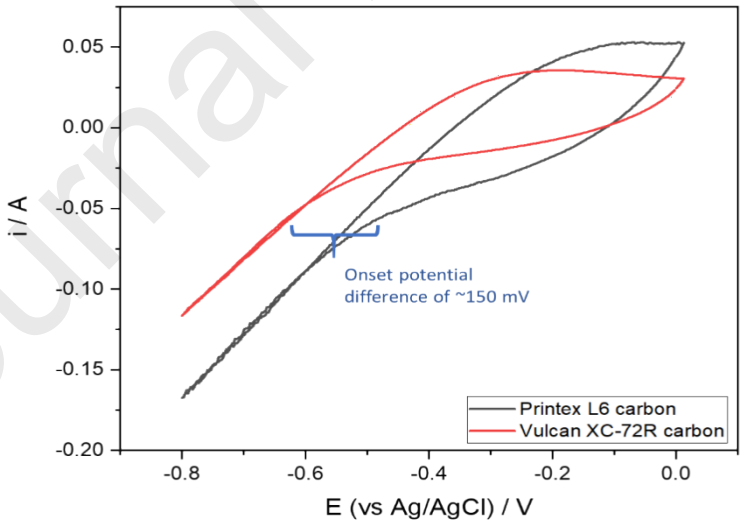

Figure 6. Cyclic voltammetry curves obtained under the potential ranging from 0.0 to -0.8 V (cathodic region) for Printex L6 carbon and Vulcan XC72 carbon. The analysis was performed using O_2-saturated 0.1 mol L^{-1} Na_2SO_4 (pH 2,5 adjusted with H_2SO_4) as electrolyte solution at scan rate of 10 mV s^{-1}.

proportional to the current value. The ECSA value was calculated by capacitive current in the non-Faradaic potential (at -0.30 V vsAg/AgCl) at different scan rates (from 2.5 to 100 mV s^{-1}) based on Equation (11) [33,34],where C_{dl} is the double layer capacitance and C_s is the capacitance of a flat surface of carbonaceous material (which corresponds to 40.0 µF cm^{-2})[41].

$$ECSA = \frac{C_{dl}}{C_s} \quad (11)$$

Based on the linear slope of Figure 7, which corresponds to the C_{dl}, we were able to estimate the ESCA of each material. Printex L6 carbon recorded C_{dl} value of 1.230 mF and ECSA value of 6.03 10^{-3} m^2 g^{-1}; while Vulcan XC-72R carbon recorded C_{dl} and ECSA values of 0.664 mF and 3.25 10^{-3} m^2 g^{-1}, respectively.

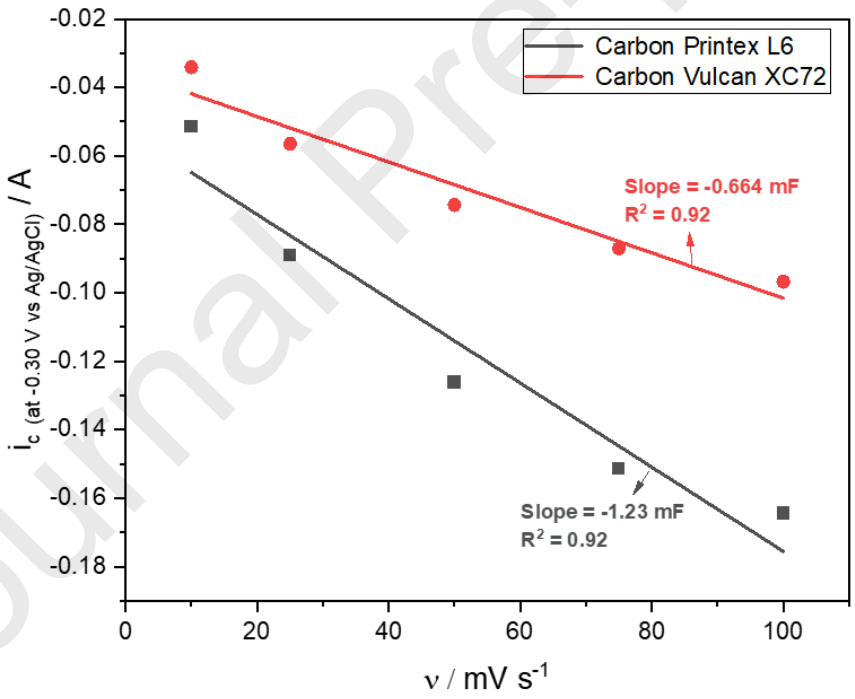

Figure 7. Average capacitive current at -0.30 V with different scan rates. O_2-saturated 0.1 mol L^{-1} Na_2SO_4 (pH 2,5 adjusted with H_2SO_4) was used as electrolyte solution.

Since the ECSA value and the amount of electrogenerated H_2O_2 recorded for the Printex L6 carbon-based GDE was 1.85 and 2.13 times higher (at 75 mA cm^{-2}) than the values obtained for the Vulcan XC-72R carbon/GDE, one can say that the efficiency of H_2O_2 generation is directly proportional to the electrochemically active surface area of the electrode.

The high efficiency of the Printex L6 carbon-based GDE, which recorded a production capacity of 4,600 mg L^{-1} of H_2O_2 in ORR via $2e^-$, can be attributed to the synergism of its high electrochemical surface area and outstanding chemical composition (presence of defects and edges on the surface, as well as oxygen-containing functional groups), which contributed toward increasing and activating ORR active sites during electrolysis.

3.3 Lifetime of PL6C/GDE and Vulcan XC-72R carbon/GDE

Durability studies were carried out in order to evaluate the resistance of the electrode against the application of a high current density (200 mA cm^{-2}) for a period of time until the E_{cell} increases exponentially; in other words, until the useful life of the electrode is reached. As can be seen in Figure 8, the Vulcan XC-72R carbon-based GDE kept its cell potential voltage constant in the potential range of 8-9 V for 25 Ah; this corresponds to approximately 5 days of uninterrupted operation. The PL6C/GDE exhibited a lifetime that was 1.8 times longer than that of the Vulcan XC-72R carbon/GDE, with maximum lifetime of 36 Ah or 7,5 days of uninterrupted operation. After the useful life of the electrode, it was observed that the electrolyte permeated through the electrode, and this caused flooding in the channels of the GDE.

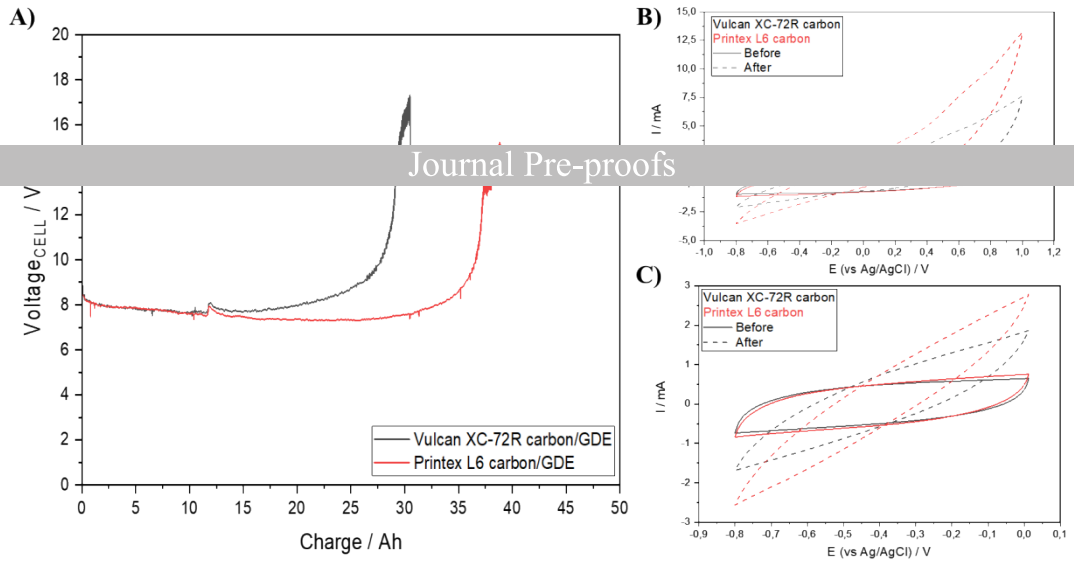

Figure 8. A) Durability tests for Vulcan XC72R carbon (black line) and Printex L6 carbon (red line) electrodes at an applied constant current density of 200 mA cm^{-2}. Cyclic voltammetry curves were obtained from **B)** +1.0 to -0.8 V and from **C)** 0.0 to -0.8 V (cathodic region) at scan rate of 50 mVs^{-1}. O_2-saturated 0.1 mol L^{-1} Na_2SO_4 (pH 2,5 adjusted with H_2SO_4) was used as electrolyte solution.

Cyclic voltammetry analyses were performed in the potential ranges between +1.0 and -0.8 V (wide range of the potential window) and between 0.0 and -0.8 V (cathode region) before and after the durability tests. Looking at Figures 8B and C, one will observe that both electrodes presented more resistive current profiles after the durability tests; this may imply that the carbon layer is being removed from the substrate. To prove the possible removal of the carbon layer from the substrate, SEM images of Printex L6 and Vulcan XC-72Rcarbon-based GDEs were obtained before and after the durability tests. Looking at the SEM images in Figure 9, one will notice that both electrodes exhibited cracked surfaces and the thickness of the crack gradually increased after use. The Vulcan XC-72R carbon-GDE exhibited a relatively more pronounced cracked surface, with complete removal of the Vulcan XC-72R carbon film on the carbon cloth substrate. With regard to Printex L6 carbon, one can still observe the presence of some regions with the carbon film on the cloth substrate.

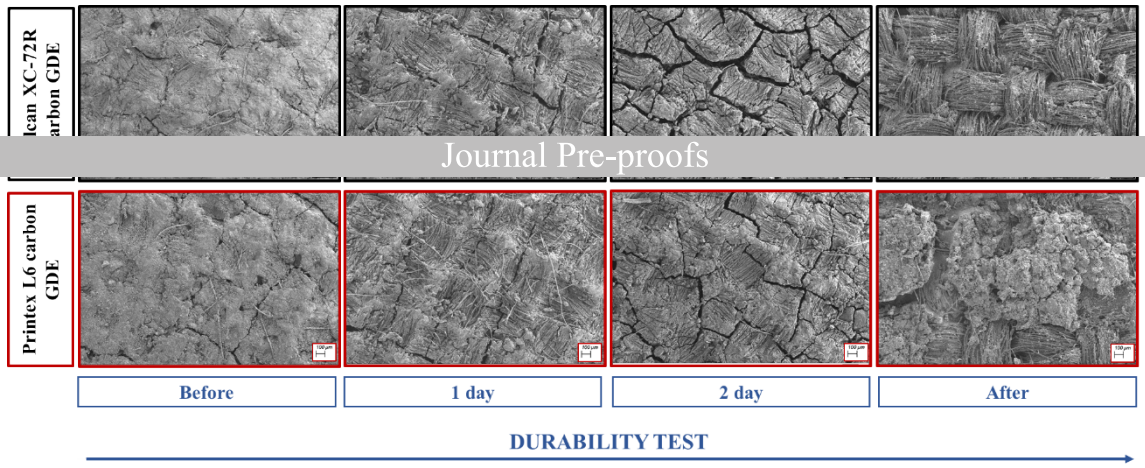

Figure 9. SEM images of Printex L6 carbon/GDE and Vulcan XC-72R carbon /GDE before and after the durability tests with 40x magnification.

4 CONCLUSIONS

The present work reported the application of a novel highly efficient and robust Printex L6 carbon-based GDE to produce H_2O_2 at high concentrations using a flow-by electrochemical reactor. The following conclusions can be drawn from the results obtained in this study:

- The PL6C/GDE led to the production of an accumulated H_2O_2 concentration of 3,913 mg L^{-1} (H_2O_2 rate of 29 mg L^{-1} min^{-1}) at 150 mA cm^{-2} in 5 h of electrolysis - this result points to a production efficiency of 17.8 g/kWh. The increase in the concentration of the predator species (ozone and persulfate) led to a decrease in H_2O_2 concentration after 5 h; however, this effect was not observed at lower current densities.
- PL6C/GDE yielded H_2O_2 concentration of 4,616 (in 12 h), 3,913 (in 5 h), and 5,032 mg L^{-1} (in 4 h) with production efficiencies of 29.5, 17.7 and 17.8 g kWh^{-1} at current densities of 75, 150 and 200 mA cm^{-2}, respectively.
- PL6C/GDE exhibited high H_2O_2 production efficiency which was 3.4–3.9 times higher than Vulcan XC-72R/GDE; This improved effect can be

attributed to its higher ECSA and the presence of higher contents of carboxyl functional groups in its composition. In addition, PL6C/GDE had a useful life of 36 Ah (7.5 days) of uninterrupted operation in acidic medium; this was 1.5 times longer than Vulcan XC-72R/GDE.

Declaration of interests

☒ The authors declare that they have no known competing financial interests or personal relationships that could have appeared to influence the work reported in this paper.

☐The authors declare the following financial interests/personal relationships which may be considered as potential competing interests:

Acknowledgements

This work is part of the research projects PID2019-107271RB-I00 funded by MCIN/ AEI/10.13039/501100011033/ and "Unión Europea Next Generation EU/PRTR". The authors warmly acknowledge the financial assistance provided by the Brazilian research funding agencies, including the Brazilian National Council for Scientific and Technological Development – CNPq (grants no. #303943/2021-1), São Paulo Research

Foundation (FAPESP – grants #2016/19612-4, #2017/10118-0, and #2020/13088-7) and the Coordenação de Aperfeiçoamento de Pessoal de Nível Superior (CAPES – Finance Code 001) in support of this research.

REFERENCES

[1] S. Siahrostami, S.J. Villegas, A.H. Bagherzadeh Mostaghimi, S. Back, A.B. Farimani, H. Wang, K.A. Persson, J. Montoya, A Review on Challenges and Successes in Atomic-Scale Design of Catalysts for Electrochemical Synthesis of Hydrogen Peroxide, ACS Catalysis. 10 (2020) 7495–7511. https://doi.org/10.1021/acscatal.0c01641.

[2] Y. Pang, H. Xie, Y. Sun, M.-M. Titirici, G.-L. Chai, Electrochemical oxygen reduction for H_2O_2 production: catalysts, pH effects and mechanisms, Journal of Materials Chemistry A. 8 (2020) 24996–25016. https://doi.org/10.1039/D0TA09122G.

[3] W. Zhou, X. Meng, J. Gao, A.N. Alshawabkeh, Hydrogen peroxide generation from O2 electroreduction for environmental remediation: A state-of-the-art review, Chemosphere. 225 (2019) 588–607. https://doi.org/10.1016/j.chemosphere.2019.03.042.

[4] Z. Pan, K. Wang, Y. Wang, P. Tsiakaras, S. Song, In-situ electrosynthesis of hydrogen peroxide and wastewater treatment application: A novel strategy for graphite felt activation, Applied Catalysis B: Environmental. 237 (2018) 392–400. https://doi.org/10.1016/j.apcatb.2018.05.079.

[5] P.A. Christensen, T. Yonar, K. Zakaria, The Electrochemical Generation of Ozone: A Review, Ozone: Science and Engineering. 35 (2013) 149–167. https://doi.org/10.1080/01919512.2013.761564.

[6] S. Mehta, D. Gupta, T.C. Nagaiah, Selective Electrochemical Production of Hydrogen Peroxide from Reduction of Oxygen on Mesoporous Nitrogen Containing Carbon, ChemElectroChem. 9 (2022). https://doi.org/10.1002/celc.202101336.

[7] P.J.M. Cordeiro-Junior, M.S. Kronka, L.A. Goulart, N.C. Veríssimo, L.H. Mascaro, M.C. dos Santos, R. Bertazzoli, M.R. de V. Lanza, Catalysis of oxygen reduction reaction for H2O2 electrogeneration: The impact of different conductive carbon matrices and their physicochemical properties, Journal of Catalysis. 392 (2020) 56–68. https://doi.org/10.1016/j.jcat.2020.09.020.

[8] Á. Moratalla, D.M. Araújo, G.O.M.A. Moura, E. Lacasa, P. Cañizares, M.A. Rodrigo, C. Sáez, Pressurized electro-Fenton for the reduction of the environmental impact of antibiotics, Separation and Purification Technology. 276 (2021). https://doi.org/10.1016/j.seppur.2021.119398.

[9] W.R.P. Barros, R.M. Reis, R.S. Rocha, M.R.V. Lanza, Electrogeneration of hydrogen peroxide in acidic medium using gas diffusion electrodes modified with cobalt (II) phthalocyanine, Electrochimica Acta. 104 (2013) 12–18. https://doi.org/10.1016/j.electacta.2013.04.079.

[10] J.F. Carneiro, R.S. Rocha, P. Hammer, R. Bertazzoli, M.R.V. Lanza, Hydrogen peroxide electrogeneration in gas diffusion electrode nanostructured with Ta2O5, Applied

Catalysis A: General. 517 (2016) 161–167. https://doi.org/10.1016/j.apcata.2016.03.013.

[11] A. Moraes, M.H.M.T. Assumpção, F.C. Simões, V.S. Antonin, M.R.V. Lanza, P. Hammer, M.C. Santos, Surface and Catalytical effects on Treated Carbon Materials for Hydrogen [illegible] https://doi.org/10.1007/s12678-015-0279-5.

[12] P.J.M. Cordeiro-Junior, R. Gonçalves, T.T. Guaraldo, R. da Silva Paiva, E.C. Pereira, M.R. de V. Lanza, Oxygen reduction reaction: Semi-empirical quantum mechanical and electrochemical study of Printex L6 carbon black, Carbon N Y. 156 (2020) 1–9. https://doi.org/10.1016/j.carbon.2019.09.036.

[13] E. Yeager, Electrocatalysts for O2 reduction, Electrochimica Acta. 29 (1984) 1527–1537. https://doi.org/10.1016/0013-4686(84)85006-9.

[14] E. Yeager, Dioxygen electrocatalysis: mechanisms in relation to catalyst structure, Journal of Molecular Catalysis. 38 (1986) 5–25. https://doi.org/10.1016/0304-5102(86)87045-6.

[15] M.A. Molina-García, N. v. Rees, Effect of catalyst carbon supports on the oxygen reduction reaction in alkaline media: A comparative study, RSC Advances. 6 (2016) 94669–94681. https://doi.org/10.1039/c6ra18894j.

[16] F. Yu, M. Zhou, L. Zhou, R. Peng, A Novel Electro-Fenton Process with H2O2 Generation in a Rotating Disk Reactor for Organic Pollutant Degradation, Environmental Science and Technology Letters. 1 (2014) 320–324. https://doi.org/10.1021/ez500178p.

[17] W. Yang, M. Zhou, J. Cai, L. Liang, G. Ren, L. Jiang, Ultrahigh yield of hydrogen peroxide on graphite felt cathode modified with electrochemically exfoliated graphene, Journal of Materials Chemistry A. 5 (2017) 8070–8080. https://doi.org/10.1039/c7ta01534h.

[18] F. Yu, M. Zhou, X. Yu, Cost-effective electro-Fenton using modified graphite felt that dramatically enhanced on H2O2 electro-generation without external aeration, Electrochimica Acta. 163 (2015) 182–189. https://doi.org/10.1016/j.electacta.2015.02.166.

[19] M. Mazzucato, C. Durante, Insights on Oxygen Reduction Reaction to H2O2: The role of functional groups and textural properties on the activity and selectivity of doped carbon electrocatalysts, Current Opinion in Electrochemistry. 35 (2022) 101051. https://doi.org/10.1016/j.coelec.2022.101051.

[20] M.K. Sales Monteiro, Á. Moratalla, C. Sáez, E.V. dos Santos, M.A. Rodrigo, Electrochemical Production of Hydrogen Peroxide in Perchloric Acid Supporting Electrolytes for the Synthesis of Chlorine Dioxide, Industrial & Engineering Chemistry Research. 61 (2022) 3263–3271. https://doi.org/10.1021/acs.iecr.1c04845.

[21] O. Garcia-Rodriguez, Y.Y. Lee, H. Olvera-Vargas, F. Deng, Z. Wang, O. Lefebvre, Mineralization of electronic wastewater by electro-Fenton with an enhanced graphene-based gas diffusion cathode, Electrochimica Acta. 276 (2018) 12–20. https://doi.org/10.1016/j.electacta.2018.04.076.

[22] V.B. Lima, L.A. Goulart, R.S. Rocha, J.R. Steter, M.R.V. Lanza, Degradation of antibiotic ciprofloxacin by different AOP systems using electrochemically generated hydrogen

peroxide, Chemosphere. 247 (2020). https://doi.org/10.1016/j.chemosphere.2019.125807.

[23] J. Moreira, V. Bocalon Lima, L. Athie Goulart, M.R.V. Lanza, Electrosynthesis of hydrogen peroxide using modified gas diffusion electrodes (MGDE) for environmental [illegible] Catalysis B: Environmental. 248 (2019) 95–107. https://doi.org/10.1016/j.apcatb.2019.01.071.

[24] W.R.P. Barros, T. Ereno, A.C. Tavares, M.R. v. Lanza, In Situ Electrochemical Generation of Hydrogen Peroxide in Alkaline Aqueous Solution by using an Unmodified Gas Diffusion Electrode, ChemElectroChem. 2 (2015) 714–719. https://doi.org/10.1002/celc.201402426.

[25] P.J.M. Cordeiro-Junior, A.S. Martins, G.B.S. Pereira, F.V. Rocha, M.A.R. Rodrigo, M.R. de V. Lanza, Bisphenol-S removal via photoelectro-fenton/H2O2 process using Co-porphyrin/Printex L6 gas diffusion electrode, Separation and Purification Technology. 285 (2022). https://doi.org/10.1016/j.seppur.2021.120299.

[26] X. Yu, M. Zhou, G. Ren, L. Ma, A novel dual gas diffusion electrodes system for efficient hydrogen peroxide generation used in electro-Fenton, Chemical Engineering Journal. 263 (2015) 92–100. https://doi.org/10.1016/j.cej.2014.11.053.

[27] A. Zadick, L. Dubau, N. Sergent, G. Berthomé, M. Chatenet, Huge Instability of Pt/C Catalysts in Alkaline Medium, ACS Catalysis. 5 (2015) 4819–4824. https://doi.org/10.1021/acscatal.5b01037.

[28] V. Ruiz, R. Santamaría, M. Granda, C. Blanco, Long-term cycling of carbon-based supercapacitors in aqueous media, Electrochimica Acta. 54 (2009) 4481–4486. https://doi.org/10.1016/j.electacta.2009.03.024.

[29] G. Acosta-Santoyo, L.F. León-Fernández, E. Bustos, P. Cañizares, M.A. Rodrigo, J. Llanos, On the production of ozone, hydrogen peroxide and peroxone in pressurized undivided electrochemical cells, Electrochimica Acta. 390 (2021). https://doi.org/10.1016/j.electacta.2021.138878.

[30] Y.-H. Wang, Q.-Y. Chen, Anodic Materials for Electrocatalytic Ozone Generation, International Journal of Electrochemistry. 2013 (2013) 1–7. https://doi.org/10.1155/2013/128248.

[31] M. Rodríguez-Peña, J.A. Barrios Pérez, J. Llanos, C. Sáez, M.A. Rodrigo, C.E. Barrera-Díaz, New insights about the electrochemical production of ozone, Current Opinion in Electrochemistry. 27 (2021). https://doi.org/10.1016/j.coelec.2021.100697.

[32] M. Rodríguez-Peña, J.A.B. Pérez, J. Llanos, C. Saez, C.E. Barrera-Díaz, M.A. Rodrigo, Understanding ozone generation in electrochemical cells at mild pHs, Electrochimica Acta. 376 (2021). https://doi.org/10.1016/j.electacta.2021.138033.

[33] L.G. de Sousa, D. v. Franco, L.M. da Silva, Electrochemical ozone production using electrolyte-free water for environmental applications, Journal of Environmental Chemical Engineering. 4 (2016) 418–427. https://doi.org/10.1016/j.jece.2015.11.042.

[34] D. Pantea, H. Darmstadt, S. Kaliaguine, C. Roy, Electrical conductivity of conductive carbon blacks: Influence of surface chemistry and topology, Applied Surface Science. 217 (2003) 181–193. https://doi.org/10.1016/S0169-4332(03)00550-6.

[35] P. Cañizares, C. Sáez, J. Lobato, R. Paz, M.A. Rodrigo, Effect of the Operating Conditions

Electrochemical Society. 154 (2007) E37. https://doi.org/10.1149/1.2424409.

[36] P.J.M. Cordeiro-Junior, J. Lobato Bajo, M.R. de V. Lanza, M.A. Rodrigo Rodrigo, Highly Efficient Electrochemical Production of Hydrogen Peroxide Using the GDE Technology, Industrial & Engineering Chemistry Research. (2022). https://doi.org/10.1021/acs.iecr.2c01669.

[37] Q. Zhang, M. Zhou, G. Ren, Y. Li, Y. Li, X. Du, Highly efficient electrosynthesis of hydrogen peroxide on a superhydrophobic three-phase interface by natural air diffusion, Nature Communications. 11 (2020). https://doi.org/10.1038/s41467-020-15597-y.

[38] Y. Lin, Q. Lu, F. Song, L. Yu, A.K. Mechler, R. Schlögl, S. Heumann, Oxygen Evolution Reaction at Carbon Edge Sites: Investigation of Activity Evolution and Structure–Function Relationships with PolycyclicAromatic Hydrocarbons, Angewandte Chemie. 131 (2019) 9010–9014. https://doi.org/0.1002/anie.201902884.

[39] Y. Bu, Y. Wang, G.F. Han, Y. Zhao, X. Ge, F. Li, Z. Zhang, Q. Zhong, J.B. Baek, Carbon-Based Electrocatalysts for Efficient Hydrogen Peroxide Production, Advanced Materials. 33 (2021). https://doi.org/10.1002/adma.202103266.

[40] R. Ma, G. Lin, Y. Zhou, Q. Liu, T. Zhang, G. Shan, M. Yang, J. Wang, A review of oxygen reduction mechanisms for metal-free carbon-based electrocatalysts, Npj Computational Materials. 5 (2019). https://doi.org/10.1038/s41524-019-0210-3.

[41] C.C.L. McCrory, S. Jung, J.C. Peters, T.F. Jaramillo, Benchmarking heterogeneous electrocatalysts for the oxygen evolution reaction, J Am Chem Soc. 135 (2013) 16977–16987. https://doi.org/10.1021/ja407115p.

[42] D. Voiry, M. Chhowalla, Y. Gogotsi, N.A. Kotov, Y. Li, R.M. Penner, R.E. Schaak, P.S. Weiss, Best Practices for Reporting Electrocatalytic Performance of Nanomaterials, ACS Nano. 12 (2018) 9635–9638. https://doi.org/10.1021/acsnano.8b07700.